

2) GMAS  $4 \times 4$ —a simple Cowell integration with  $4 \times 4$  geopotential field, no third-body perturbations, and no atmospheric drag.

3) OrbJ2—a personal computer version of the two-body propagator described in this paper.

4) Fastorb—a personal computer-based algorithm similar to OrbJ2 but omitting the mean-to-osculating transformation of the semimajor axis.

The results of these runs are included in Table 1 and Figs. 1 and 2. The intrack, or longitude, error is clearly the dominant error. The error in GMAS  $4 \times 4$  and OrbJ2 is due to the neglect of drag; the larger error in Fastorb is due to the error of order  $J_2$  in the computation of the mean motion.

As an example of the resolution available in computer displays, we consider the IBM Enhanced Graphics Adaptor (EGA) board, which is widely used in personal computers. The resolution of the EGA board is  $640 \times 350$  pixels (horizontal by vertical). Given that the entire world map is displayed (i.e.,  $-180^\circ$  longitude to  $180^\circ$  longitude and  $-90^\circ$  latitude to  $90^\circ$  latitude) the number of pixels per degree of longitude is

$$(640/360) = 1.78 \text{ pixels/longitude degree}$$

and the number of pixels per degree of latitude is

$$(350/180) = 1.94 \text{ pixels/latitude degree}$$

In the case of this orbit scenario, the position of the Hubble Space Telescope after one week using OrbJ2 orbit propagator would have an error of

$$0.94^\circ \text{ longitude} = 1.67 \text{ pixels} = 0.26\% \text{ of the world map width}$$

$$0.08^\circ \text{ latitude} = 0.16 \text{ pixels} = 0.04\% \text{ of the world map height}$$

Note that these graphics screen errors are with respect to the position of the spacecraft subsatellite point. If a zoom is applied to the world map projection, the pixel and screen error becomes greater. In any case, the errors are quite acceptable for graphical display.

### Conclusions

A fast, simple, analytic orbit propagator has been developed and shown to give acceptable results for the graphical display of the trajectories of Earth-orbiting satellites. First-order effects of the oblateness of the Earth on the orbit are included in a consistent manner. In particular, the propagator includes a mean-to-osculating transformation on the semimajor axis because large intrack errors can result from ignoring the distinction between mean and osculating values of this parameter.

### Acknowledgment

The authors would like to thank Bob Dasenbrock of the U.S. Naval Research Laboratory for explaining the large intrack errors in analytic orbit theories that ignore the distinction between mean and osculating elements.

### References

- Breakwell, J. V., and Vagners, J., "On Error Bounds and Initialization in Satellite Orbit Theories," *Celestial Mechanics*, Vol. 2, No. 2, 1970, pp. 253-264.
- Roy, A. E., *Orbital Motion*, Adam Hilger, Bristol, England, UK, 1982.
- Cappelari, J. O., Jr., Velez, C. E., and Fuchs, A. J. (eds.), *Mathematical Theory of the Goddard Trajectory Determination System*, NASA-X-582-76-77, April 1976.

## Adaptive Noise Models for Extended Kalman Filter

K. Kumar,\* D. Yadav,† and B. V. Srinivas‡  
Indian Institute of Technology, Kanpur, 208 016 India

### Introduction

KALMAN filters are sensitive to modeling errors as well as input statistics.<sup>1-3</sup> The danger of degradation in numerical performance is associated with the weakening/loss of positive definiteness of state covariance, leading to poorer predictions. The problem is further aggravated by measurement bias and relatively large errors in the starting state estimates.<sup>4,5</sup> Here, an attempt is made to develop a "global" extended Kalman filter by introducing some suitable adaptive driving noise covariance models. Numerical simulation of the problem of satellite orbit estimation from observational data using this filter with the proposed noise models clearly establishes their efficacy.

To combat the filter divergence, it is necessary to adopt schemes that ensure positive definiteness of the state covariance matrix and prevent it from "diminishing too rapidly."

Several trial and error approaches incorporating varying amounts of fictitious driving noise have been proposed<sup>4,6</sup>; however, these normally require a large number of simulation trials. Furthermore, the success of the filter is strongly dependent on errors in the initial state estimates assumed, thus leaving a degree of unpredictability regarding the filter convergence. Here, attention is focused on developing the noise models that would ensure filter convergence irrespective of the initial state estimate errors to the extent possible.

### Adaptive State Noise Models

The models proposed here are dependent on some suitable measures of the state errors. These measures are taken to be residuals that are nothing but the differences between the actual observation values and their corresponding numerically "computed" projections. Numerous schemes were tried, of which only some are presented. Efficacy of the proposed models is tested through a problem of satellite orbit determination using an extended Kalman filter algorithm. The noise models presented here can be classified into two broad categories, as discussed in the following.

#### Noise Models Based on Observation Residuals

Here, we assume the driving noise covariance matrix  $Q$  to be diagonal; it is constructed using the observation residual statistics. It was felt that the diagonal terms should be taken so as to represent the level of dispersion in the corresponding observations. To account for systematic modeling errors, on the other hand, a certain degree of dependence of these terms on the means of observations also appears natural. It is therefore proposed to develop models with diagonal entries in  $Q$  based on the means as well as the standard deviations of the observation residuals. This has been incorporated such that an increase in systematic errors, reflected by enlarged mean errors, promotes fading memory, whereas the growth in the standard deviation induces expanding filter memory. It is therefore hoped that the following models proposed here would pave the way for adaptive filter characteristics.

Presented as IAF Paper 88-305 at the 39th IAF Congress, Bangalore, India, Oct. 1988; received Aug. 3, 1989; revision received Nov. 1, 1989. Copyright © 1990 by the Authors. Published by the American Institute of Aeronautics and Astronautics, Inc., with permission.

\*Professor, Department of Aerospace Engineering. Associate Fellow AIAA.

†Assistant Professor, Department of Aerospace Engineering.

‡Former Graduate Student, Department of Aerospace Engineering.

Model 1:

$$Q_{ij} = \begin{cases} 0 & ; i \neq j \\ |c_1 \mu_{\Delta \rho} - c_2 \sigma_{\Delta \rho}| & ; i = j = 1, 2, 3 \\ |c_1 \mu_{\Delta \dot{\rho}} - c_2 \sigma_{\Delta \dot{\rho}}| & ; i = j = 4, 5, 6 \end{cases}$$

Model 2:

$$Q_{ij} = \begin{cases} 0 & ; i \neq j \\ |c_1 \mu_{\Delta \rho} - d \sqrt{c_1} \sigma_{\Delta \rho}| e & ; i = j = 1, 2, 3 \\ |c_1 \mu_{\Delta \dot{\rho}} - d \sqrt{c_2} \sigma_{\Delta \dot{\rho}}| & ; i = j = 4, 5, 6 \end{cases}$$

Model 3:

$$Q_{ij} = \begin{cases} 0 & ; i \neq j \\ |c_1 \mu_{\Delta \rho} - c_2 \sigma_{\Delta \rho}^2| & ; i = j = 1, 2, 3 \\ |c_1 \mu_{\Delta \dot{\rho}} - c_2 \sigma_{\Delta \dot{\rho}}^2| & ; i = j = 4, 5, 6 \end{cases}$$

where

$$\begin{aligned} d &= (1 + c_2/k_1) \\ e &= \text{scale factor; } [\Delta \rho / (200 \Delta \dot{\rho})] \text{ subject to } 1 \leq e \leq 10 \\ \Delta \rho, \Delta \dot{\rho} &= \text{observation residuals in range } \rho \text{ and range rate } \dot{\rho}, \text{ respectively} \end{aligned}$$

The constants  $c_1$  and  $c_2$ , which we refer to as noise participation constants, are chosen by trial and error.

The success of these models depends considerably on the choice of constants  $c_1$  and  $c_2$ . Some numerical trials are initially needed to arrive at the best values of these constants for the problem at hand.

#### Noise Model Based on Vibration Damping Analogy

Here, "damping" is artificially introduced by varying the driving noise covariance matrix drawing inspiration from the concept of viscous damping in vibrating systems. The damping role is assigned to noise covariance by making its diagonal entries proportional to the rate of change of residuals in the corresponding state variable while the off-diagonal terms in covariance are set to zero. Thus, this model is constructed as follows:

Model 4:

$$Q_{ij} = \begin{cases} 0 & ; i \neq j; i, j = 1, 2, \dots, 6 \\ |\Delta x_i \cdot \Delta \dot{x}_i| \Delta t & ; i = j \end{cases}$$

where

$$\begin{aligned} \Delta x_i &= \text{computed state residuals} \\ \Delta \dot{x}_i &= \text{time derivative of state residuals, computed numerically through curve fitting} \\ \Delta t &= \text{step size on time} \end{aligned}$$

The term  $\Delta t$  has been introduced in  $Q_{ij}$  with a view to achieving dimensional consistency.

### Results and Discussion

Efficacy of the proposed noise models is tested through the problem of satellite orbit estimation from simulated observational data. The results are presented for the observational data generated every second for a single ground station with

Table 1 Statistics of observation data considered

Observed variable	Standard deviation	Bias
Range, $\rho$	30 m	$\pm 30$ m
Range rate, $\dot{\rho}$	0.1 m/s	$\pm 0.3$ m/s
Azimuth	0.03 deg	$\pm 0.1$ deg
Elevation	0.03 deg	$\pm 0.1$ deg

Table 2 Filter performance: model 1 ( $c_1 = 10^{-5}$ ,  $c_2 = 10^{-4}$ )

Case number		Time, s					
		0	20	40	60	80	100
1	Position error, km	10.0	8.2	8.3	7.8	6.8	5.1
	Velocity error, m/s	50.0	39.9	38.0	33.2	24.6	13.0
2	Position error, km	100.0	36.3	12.2	8.4	4.9	4.1
	Velocity error, m/s	5.0	8.9	6.7	4.1	2.1	2.2
3	Position error, km	100.0	35.7	12.7	8.4	4.5	4.6
	Velocity error, m/s	0.5	9.6	7.0	4.1	2.0	2.7
4	Position error, km	1.0	0.7	0.7	0.6	0.5	0.4
	Velocity error, m/s	0.5	0.4	0.4	0.4	0.3	0.3

Table 3 Filter performance: damping noise model

Case number		Time, s					
		0	20	40	60	80	100
1	Position error, km	34.5	0.1	0.2	0.1	0.1	0.1
	Velocity error, m/s	50.5	14.3	26.5	11.1	4.2	3.5
2	Position error, km	69.4	0.1	0.2	0.1	0.1	0.1
	Velocity error, m/s	103.0	7.9	15.6	6.2	1.2	1.0
3	Position error, km	105.2	0.1	0.4	0.2	0.1	0.0
	Velocity error, m/s	171.0	47.5	18.9	35.1	3.3	1.2
4	Position error, km	140.6	0.1	0.3	0.1	0.1	0.1
	Velocity error, m/s	214.4	18.2	17.9	0.2	0.8	0.5
5	Position error, km	176.9	0.0	0.1	0.1	0.1	0.1
	Velocity error, m/s	273.7	16.0	29.0	3.8	2.0	1.7

Table 4 Influence of varying the initial state covariance matrix  $P_0$  on filter performance: damping noise model

Multiplying factor		Time, s					
		0	20	40	60	80	100
0.001	Position error, km	105.2	0.2	0.1	0.1	0.0	0.0
	Velocity error, m/s	171.0	333.8	16.8	16.1	6.8	1.6
0.01	Position error, km	105.2	0.0	0.0	0.1	0.0	0.0
	Velocity error, m/s	171.0	101.3	4.5	3.2	2.4	1.4
0.1	Position error, km	105.2	0.2	0.0	0.0	0.0	0.0
	Velocity error, m/s	171.0	633.2	10.7	10.4	5.7	1.4
1.0	Position error, km	105.2	0.1	0.4	0.1	0.1	0.0
	Velocity error, m/s	171.0	47.5	18.9	35.1	3.3	1.2
10.0	Position error, km	105.2	0.2	0.1	0.1	0.0	0.0
	Velocity error, m/s	171.0	306.0	36.0	4.0	2.1	1.1
100.0	Position error, km	105.2	0.0	0.0	0.1	0.0	0.0
	Velocity error, m/s	171.0	80.2	4.0	3.6	2.3	1.7
1000.0	Position error, km	105.2	0.1	0.0	0.0	0.0	0.0
	Velocity error, m/s	171.0	261.6	17.5	8.4	4.0	1.1

the statistics given in Table 1. The results include cases with several error levels in the initial state vector assumed.

The simulation results with the noise of model 1 based on observation residuals are presented in Table 2.

Using model 1, together with a proper choice of constants  $c_1$  and  $c_2$ , the filter seems capable of handling the large initial errors. The accuracy of the estimates obtained is, however,

dependent on the level of bias present in the data, as expected. It may be emphasized that once the appropriate constants have been ascertained, no further trials are required, thus facilitating its use in real time processing of data.

Similarly, the other two observation residual-based models can also be effectively used in processing data. It was found that by using these models in various suitable sequential combinations, it is possible to significantly improve the resulting accuracy.

Finally, we present the results of simulation runs with noise model 4, which is based on vibration damping analogy. Table 3 shows filter runs with different initial errors in the position and velocity estimates. It is evident that the proposed filter is able to control the errors to within a much lower level rather quickly. With the filter progressing further in time, the error levels continue to fall, leading to an accurate satellite orbit estimation. It is interesting to note that this fast filter convergence is achieved in all cases regardless of the error levels in the initial guess.

The initial state covariance  $P_0$  is not known a priori and has to be "guesstimated." In general, the filter performance is dependent on the accuracy of this guess as well. To assess the sensitivity of the noise model to the initial state covariance, the filter performance was evaluated for varying  $P_0$ . For filter runs, its base values were adopted from the corresponding elements of the observation noise covariance  $R$ . The results of this study with  $P_0$  varied over several orders of magnitude are presented in Table 4. It can be seen that a rather rapid rate of convergence achieved by the filter remains virtually unaffected by the assumed values of the covariance  $P_0$ . It clearly establishes the importance of the proposed noise model in providing the self-adaptive filter characteristics and fast convergence, even under the most adverse situations. Thus, the mechanization of the last model appears to be not only independent of the initial guess of the state vector but also the state covariance. It is computationally more rugged as well as reliable and enables convergence in all cases tested. Furthermore, there being no constants here, unlike in the earlier three models, no tuning is required whatsoever.

### Concluding Remarks

Presented here are four adaptive driving noise covariance models with a view to combat the filter divergence problems in implementation of the Kalman filter. The first three models are based on statistics of the observation residuals. These appear to make the filter quite robust, being effective regardless of the level of state errors in the initial guess. However, these require some trials to determine the proper noise participation constants. At times, reruns may have to be resorted to for achieving higher accuracies. However, the last noise model based on vibration damping analogy is fully robust. It appears to be totally insensitive to the initial state assumed. With no need for tuning the filter or even reruns, its versatility is clearly established.

### References

- <sup>1</sup>Bierman, G. J., and Thornton, C. L., "Numerical Comparison of Kalman Filter Algorithms: Orbit Determination Case Study," *Automatica*, Vol. 13, No. 1, 1977, pp. 23-35.
- <sup>2</sup>Kumar, K., and Yadav, D., "Preliminary Orbit Determination Using Filtering Techniques: An Overview," *Proceedings of the IISc-ISRO Workshop-Cum Seminar on Preliminary Orbit Determination*, Jan. 1985, pp. 5.1.1-5.1.15.
- <sup>3</sup>Anderson, B. D. O., and Moore, J. B., *Optimal Filtering*, edited by T. Kailath, Prentice-Hall, Englewood Cliffs, NJ, 1979.
- <sup>4</sup>Morrison, N., *Introduction to Sequential Smoothing and Prediction*, McGraw-Hill, New York, 1969.
- <sup>5</sup>Gelb, A. (ed.), "Optimal Linear Filtering," *Applied Optimal Estimation*, MIT Press, Cambridge, MA, 1974.
- <sup>6</sup>Jazwinski, A. H., *Stochastic Process and Filtering Theory*, Academic, New York, 1970.

## New Star Identification Technique for Attitude Control

B. V. Sheela,\* Chandra Shekhar,\*  
P. Padmanabhan,† and M. G. Chandrasekhar‡  
Indian Space Research Organization Satellite Centre,  
Bangalore, 560 017 India

### I. Introduction

**P**RECISION pointing requirements are becoming one of the key features of many present day spacecraft. A star sensor, with<sup>1</sup> or without gyro,<sup>2</sup> is the answer to these stringent demands. For star sensor-based attitude determination, be it post facto or realtime, it is mandatory to identify the stars before attitude estimation can be carried out. In Ref. 3, Gottlieb has provided a comprehensive discussion of several star identification techniques: 1) direct match, 2) angular separation/phase match, and 3) discrete attitude variation.

The direct match technique, which associates a cataloged star with each observation by picking the closest star lying within a specified neighborhood of the observation transformed into the estimated celestial coordinates, requires that the initial attitude estimate be close to the true attitude. In the absence of a close initial estimate, the method requires accurate magnitude information for the imaged stars to resolve the problem of multiple candidate stars. By far, the angular separation technique, which matches the angular distances between pairs of imaged stars with those of cataloged stars, is the most widely used technique.<sup>4</sup> However, if the number of candidate stars is large, the method can run into ambiguities and misidentifications. The phase match technique is essentially a one-dimensional version of the angular separation technique and is suitable for spin-stabilized spacecraft. The discrete attitude variation technique, which is recommended as only a last resort by Gottlieb,<sup>3</sup> as it is essentially a method that repeatedly uses any of the techniques just mentioned for a host of attitude guesses, is very costly in terms of processing time. In this Note, yet another technique is presented that was the outcome of an

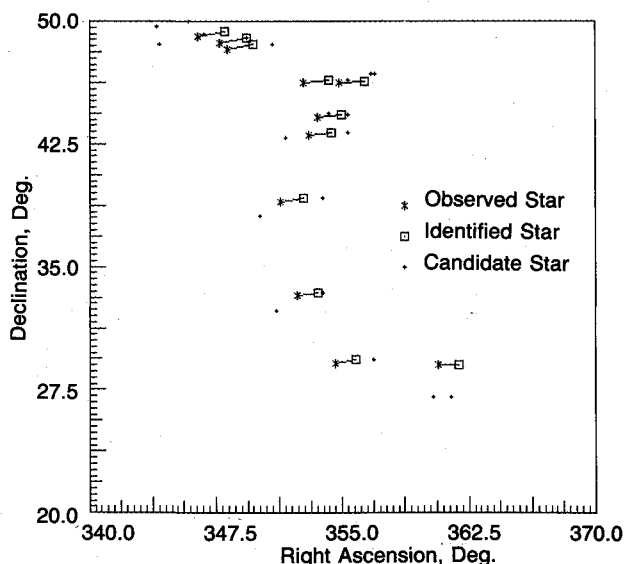


Fig. 1 Observed and candidate stars.

Received June 12, 1989; revision received Oct. 16, 1989. Copyright © 1990 by the American Institute of Aeronautics and Astronautics, Inc. All rights reserved.

\*Scientist, Flight Dynamics Division.

†Division Head, Flight Dynamics Division.

‡Scientific Secretary.